THE JOURNAL OF BIOLOGICAL CHEMISTRY VOL. 288, NO. 11, pp. 7930–7941, March 15, 2013

Tumor-derived Mutations in the Gene Associated with Retinoid Interferon-induced Mortality (GRIM-19) Disrupt Its Anti-signal Transducer and Activator of Transcription 3 (STAT3) Activity and Promote Oncogenesis*[S]

Received for publication, November 28, 2012, and in revised form, February 5, 2013 Published, JBC Papers in Press, February 5, 2013, DOI 10.1074/jbc.M112.440610

Shreeram C. Nallar[‡], Sudhakar Kalakonda[‡], Daniel J. Lindner[§], Robert R. Lorenz[¶], Eric Lamarre[¶], Xiao Weihua[‖], and Dhananjaya V. Kalvakolanu[‡1]

From the [‡]Department of Microbiology and Immunology, Program in Oncology, Greenebaum Cancer Center, University of Maryland School of Medicine, Baltimore, Maryland 21201, the [§]Taussig Cancer Center, [¶]Head and Neck Institute, Cleveland Clinic Foundation, Cleveland, Ohio 44195, and [‖]University of Science Technology, 230027 Hefei, China

Background: Aberrantly active STAT3 promotes tumorigenesis. GRIM-19 binds to STAT3 and inhibits its growth promotion.
Results: We identified three mutations in the GRIM-19 gene that failed to block STAT3-dependent gene expression and tumor development.
Conclusion: GRIM-19 mutations unleash STAT3 activity to promote tumor growth.
Significance: This study identifies a new mechanism by which normal cells acquire cancerous properties.

The signal transducer and activator of transcription 3 (STAT3) protein is critical for multiple cytokine and growth factor-induced biological responses *in vivo*. Its transcriptional activity is controlled by a transient phosphorylation of a critical tyrosine. Constitutive activation of STAT3 imparts resistance to apoptosis, promotes cell proliferation, and induces *de novo* micro-angiogenesis, three of the six cardinal hallmarks of a typical cancer cell. Earlier we reported the isolation of GRIM-19 as a growth suppressor using a genome-wide expression knockdown strategy. GRIM-19 binds to STAT3 and suppresses its transcriptional activity. To understand the pathological relevance of GRIM-19, we screened a set of primary head and neck tumors and identified three somatic mutations in *GRIM-19*. Wild-type GRIM-19 suppressed cellular transformation by a constitutively active form of STAT3, whereas tumor-derived mutants L71P, L91P and A95T significantly lost their ability to associate with STAT3, block gene expression, and suppress cellular transformation and tumor growth *in vivo*. Additionally, these mutants lost their capacity to prevent metastasis. These mutations define a mechanism by which STAT3 activity is deregulated in certain human head and neck tumors.

Aberrant growth promotion occurs because of the inactivation of tumor suppressors and activation of oncogenes. Classical tumor suppressors such as p53, pRB, and PTEN are frequently mutated in many human tumors. The Hanahan-Weinberg model (1) suggests that at least 10 different genetic and physiologic alterations occur in a mammalian cell before reaching the full-blown malignant state. These include resistance to apoptosis, enhanced motility, development of neovasculature, activation of tumor-proliferating inflammation, and loss of anti-tumor immunity. Several of these processes are dependent on cytokines and/or other secretory factors.

The interferon (IFN) family of cytokines is a critical player in promoting host defenses against pathogens and neoplastic cells (2). Unlike many other cytokines, which primarily attack the tumor through activation of immune cells, IFNs not only activate direct growth-suppressive gene expression in the tumor cells but also activate immune cells (3). Their direct anti-tumor effects include the inhibition of cell cycle and activation of apoptosis. A number of tumor suppressor genes such as STAT1 (4), IRF1 (5), IRF7 (6), IRF8 (7), and DAPK1 (8) were discovered originally as critical players in IFN action. That endogenous IFNs act as sentinels against tumors (9), many cell types are capable of producing and responding to IFNs; and the fact that most of the above proteins are transcription factors it is likely that we have not fully uncovered the tumor-suppressive gene spectrum controlled by these cytokines. In addition, we and others have shown that IFN in association with other biological response modifiers, such as retinoic acid, exhibit potent tumor suppression in several clinical and preclinical models (2). To investigate the underlying mechanisms of tumor growth suppression, we employed a genome-wide knockdown strategy and identified few potent growth suppressors. One such growth inhibitor was GRIM-19, a novel protein whose depletion promoted and overexpression suppressed tumor growth (10, 11). GRIM-19 targets STAT3 to inhibition via a direct interaction (12, 13).

STAT3 was originally identified as a cytokine-inducible transcription factor whose activity was critical for embryonic development and differentiation (14). In normal resting cells, STAT3 is transiently activated via tyrosyl phosphorylation by the JAK

* This work was supported, in whole or in part, by National Institutes of Health Grant R01 CA105005 (to D. V. K.). This work was also supported by an intramural award from the Cigarette Restitution Funds of the University of Maryland Greenebaum Cancer Center (to D. V. K.).
[S] This article contains supplemental Table S1 and Figs. S1—S4.
[1] To whom correspondence should be addressed. Tel.: 410-328-1396; E-mail: dkalvako@umaryland.edu.

family of protein-tyrosine kinases upon specific ligand-receptor engagement, which causes STAT3 homo-dimerization, nuclear migration, and transcriptional induction of target genes (14). Excessive STAT3 phosphorylation is prevented by cessation of JAK activity and nuclear export of active STAT3 (14). In contrast, STAT3 is highly active and is primarily found in the nucleus of a number of human tumors. Consistent with these observations, an experimentally generated spontaneously dimerizing STAT3 transforms cells to an oncogenic state (15). STAT3 meets at least 5 of the 10 criteria of the Hanahan-Weinberg model of tumorigenesis such as promotion of proliferation and neoangiogenesis, resistance to apoptosis, evasion of immune response, and development of tumor-promoting inflammatory response (16). Although STAT3 tyrosyl phosphorylation is one important step in growth promotion, mechanisms that deregulate STAT3 activity are far from clear, as mutations in STAT3 are not reported in human tumors to date. Therefore, we hypothesized that inactivation of STAT3 inhibitors is an important event in promoting tumor growth.

Earlier we showed that expression of GRIM-19 is suppressed in a number of primary renal cell carcinomas (10). Whether GRIM-19 mutations occur in human tumors is unclear at this stage. Here we show that the GRIM-19 gene is mutated in primary human head and neck cancers. We also show that the tumor-derived mutants fail to counteract the growth-promoting effects of STAT3 and are ineffective at suppressing metastasis due to their weak binding to STAT3. These studies not only show a new way tumor cells lose control over STAT3 but also highlight the importance of GRIM-19 mutations in tumor development.

EXPERIMENTAL PROCEDURES

Antibodies—Antibodies specific for FLAG (Sigma) and Myc (Cell signaling technology) epitopes, actin (Sigma), and cyclin D1, Bcl2, and MMP-9 (Santa Cruz Biotechnology) were used in these studies. Alexa fluor 700-coupled anti-rabbit IgG and Alexa fluor 750-coupled anti-mouse IgG (Invitrogen) were used to capture specific signals using the Odyssey Infrared system (LI-COR), and band intensities were quantified using the manufacturer's software.

Tumor Tissues—Tumors were collected with informed consent of the patients undergoing surgical excision at the Cleveland Clinic under an institutionally approved protocol. Adjacent normal tissue was used as a control in each case. Samples were snap-frozen in liquid N_2 and then stored at −80 °C until use. Total RNA and genomic DNA were isolated from these samples using a commercially available Allprep DNA/RNA/Protein mini kit (Qiagen, Inc.). Total RNA was converted to cDNA using SuperScript® III reverse transcriptase (Invitrogen) and used templates for qualitative and quantitative PCR using gene-specific primers (supplemental Table S1). *GRIM-19* ORF from tumor and normal tissue was PCR-amplified and sequenced at the Biopolymer/Genomics core facility, University of Maryland School of Medicine, Baltimore, MD. Base changes, if any, were verified using matched genomic DNA as the background. The presence or absence of such base changes in the matched normal tissue was used to score changes as germ line or somatic origin, respectively.

Expression Vectors—A FLAG-tagged spontaneously dimerizing STAT3 variant (S3C) has been described (15), and transfected cells were selected with G418. Tumor-derived GRIM-19 mutant ORFs were expressed as C-terminal myc-tagged protein using the pLVX-Puro expression vector (Clontech, Inc). Preparation of lentiviral particles were as per our earlier reports. Briefly, medium from the cultures were collected for 3 consecutive days, pooled, passed through a 0.45-μm filter, and used to transduce target cell lines.

Establishment of Cell Lines—3Y1, a non-oncogenic rat fibroblast cell line (JCRB0734, Japanese Collection of Research Bioresources, Osaka, Japan) (17), was grown in DMEM supplemented with 5% FBS, 100 units/ml penicillin, and 100 mg/ml streptomycin. This cell has two point mutations (K130T and A136T) in one of the p53 alleles (18). These mutations do not belong to the category of "hotspot mutations" observed in human tumors that destroy its DNA binding capacity (19). HaCaT (non-oncogenic keratinocytes) was grown in DMEM supplemented with 10% FBS. HSC3 cells (human oral squamous carcinoma cell line) was grown in DMEM supplemented with 10% FBS; this cell line harbors mutant the p53 allele(s). PC3 cells (prostate cancer cell line) were grown in minimum Eagle's medium supplemented with 10% FBS, glutamine, and sodium pyruvate. Cells were electroporated with the S3C expression plasmid using the Nucleofector® technology (Amaxa, Inc.). After transfection with the genes of interest, cells were selected with G418 (1500 μg/ml) for 10–12 days. Drug-resistant colony pools ($n > 50$) were expanded to avoid a clonal bias and transduced with lentiviral GRIM-19 and selected with puromycin. Expression-positive population was used in all experiments. A lentiviral luciferase reporter (pCCL-c-MNDU3c-Luc) (20) was used to transduce cells and monitor metastasis in real time.

Gene Expression Analyses—Total RNA (5 μg) was reverse-transcribed using a commercially available ImProm-II enzyme (Promega). Quantitative RT-PCR was performed using Jump-Start SYBR Green master mix (Sigma) on Stratagene Mx3005P real-time PCR machine. Input cDNA was 10 ng per reaction, and relative transcript abundance was calculated using *RPL32* as the internal control by the ΔΔCt method. For all cell line-based experiments, three separate batches of RNA ($n = 3$) were employed for a sample. Multiple technical replicates per sample were used for calculating transcript levels, and the statistical significance of differences between various groups was assessed using Student's *t* test.

Soft Agar Colony Formation, in Vitro Wound Healing, and Cell Migration Assays—These were performed as described in our previous publications (21). Chromatin immunoprecipitation (ChIP) analyses were performed as described earlier (21).

Tumorigenic Assays—Three- to four-week-old athymic nude (*nu*/*nu*) NCr mice (Taconic) were used for these studies as described earlier (22). Procedures involving animals were conducted in conformity with an institutionally approved protocol compliant with United States National Institutes of Health policies. Each experimental group contained 10 mice, with 1 tumor injection site per mouse. Cells (1×10^6) were inoculated into flanks, and tumor development was monitored for several weeks. Every week, tumor volume was calculated using caliper

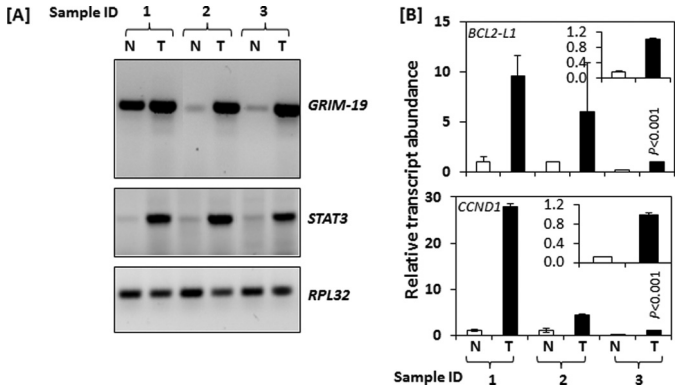

FIGURE 1. **Expression of *GRIM-19*, *STAT3*, and STAT3-regulated genes in primary oral cancers.** *A*, RT-PCR analysis of *GRIM-19* and *STAT3* transcripts from three independent samples is shown. Ribosomal protein L32 (*RPL32*) was used as an internal control. Patient samples from which specific mutants were isolated are indicated *above the panel*. *N*, normal; *T*, tumor. *B*, real-time PCR analysis of the indicated STAT3-regulated genes from samples are shown. *Insets* shows sample ID 3. These samples had a lower abundance of the RNA compared with other samples and hence were plotted separately to show the differences. *p* value was calculated by comparing normal *versus* tumor data. *Error bars* indicate S.D.

measurements and the formula $V = (4/3)\pi a^2 b$, where $2a$ = minor axis, and $2b$ = major axis of prolate spheroid. Student's two-tailed *t* test was used to assess the statistical significance of difference between pairs of means of tumor volume. For metastasis experiments, after laparotomy, 5×10^5 PC3 cells in 10 μl were inoculated into the ventral lobe of the prostate gland using a 27-gauge needle. These cells also carried a stably integrated firefly luciferase gene, which permits live imaging. Animals were monitored for metastasis after 45 days using the Xenogen IVS100 live imaging system. Mice were anesthetized with inhaled isoflurane and administered 3 mg of luciferin intraperitoneally 5 min before imaging. Image acquisition settings were: Bin 8, FOV25, f1, 30-s exposure, background subtracted, flat-fielded, cosmic.

Statistical Analyses—Data obtained with each mutant were subjected to Student's *t* test with respect to wild-type GRIM-19. Effects of wild-type GRIM-19 on S3C were compared with corresponding data from S3C/EV cells. A p value <0.05 was considered significant in all experiments.

RESULTS

Identification of Mutations in GRIM-19 in Human Oral Squamous Cell Carcinomas—We recently obtained several primary human oral squamous cell carcinomas ($n = 12$) and adjacent normal tissues from patients who were tobacco chewers. Total RNA and genomic DNA were isolated from pathologist-certified surgically isolated tumors and the adjacent normal tissues. RT-PCR analysis showed *GRIM-19* mRNA levels in some of these tumors was lower compared with their matched normal tissue, whereas there was no significant difference in others. Three of these tumors (from different patients and arbitrarily named as sample IDs 1, 2, and 3) selected for this study had higher GRIM-19 than their normal counterparts (Fig. 1*A*, *top blot*). Based on our previous studies that showed a loss of GRIM-19 correlates with elevated STAT3 levels in clear cell renal cell carcinomas (10), we expected lower *STAT3* mRNA levels in these tumors compared with their control. Contrary to this notion, *STAT3* mRNA levels were very high compared with their matched normal tissue (Fig. 1*A*, *middle blot*). Real-time PCR analysis (Fig. 1*B*) of two STAT3-regulated genes, *BCL2-L1* (BCL-XL) and *CCND1* (cyclin D1), showed increased expression, which was consistent with elevated *STAT3* levels. Based on this confounding observation that high *GRIM-19* levels in a tumor corresponded to an increased STAT3 activity, we hypothesized that the *GRIM-19* in these tumors may have suffered mutation and consequently lost its anti-STAT3 activity. Therefore, we sequenced the *GRIM-19* cDNA and genomic DNA from the selected tumors and their matched normal tissues. These studies identified three separate point mutations in the tumor *GRIM-19* gene but not in those of normal cells (supplemental Fig. S1). Because these mutations were absent in the matching normal tissues, they truly appear to be tumor-derived and somatic in nature. Each mutation was identified from a tumor derived from one patient. Within the given tumor, the mutant GRIM-19 ORF appears to be the dominant form. No other mutations were observed in the same tumor. These mutations resulted in the following amino acid substitutions in the coding region: L71P (Fig. 1 sample ID 2), L91P (Fig. 1 sample ID 1), and A95T (Fig. 1 sample ID 3). Because the available patient sample size is smaller, we could not determine the frequency of their occurrence at this time.

Tumor-derived GRIM-19 Mutants Fail to Suppress STAT3-induced Cell Growth—We first determined if the GRIM-19 mutants had an effect on the growth of non-oncogenic cells. We infected 3Y1, a non-oncogenic rodent fibroblast cell line, with lentiviral particles expressing wild-type GRIM-19 and the tumor-derived mutants, and stable cell lines were isolated by selecting with puromycin. The growth profiles of cells expressing mutants were compared with those expressing wild-type GRIM-19 (supplemental Fig. S2). The mutants did not significantly stimulate cell growth compared with wild-type GRIM-19, except for A95T, which seemed to slow down cell growth slightly. Thus, mutants seem not to differ significantly from wild-type GRIM-19 in terms of their effects on normal cell growth.

Because GRIM-19 is an inhibitor of STAT3, we next determined the impact of these mutations on STAT3-induced cell growth. A constitutively active form of STAT3 (S3C) was stably transfected into 3Y1 cells, which is known to cause oncogenic transformation. Because S3C is the only oncogenic product under these conditions, the anti-STAT3 effects of GRIM-19 and its mutants can be readily discerned using this model. Stable cell pools expressing S3C were generated after selecting cells with G418 followed by GRIM-19 transduction via lentiviral particles and selection with puromycin. First, we wanted to ascertain whether the mutants differ from wild-type GRIM-19 in regulating cell growth in the presence of the S3C oncogene. S3C alone stimulated cell growth, which was strongly suppressed by wild-type GRIM-19 ($p < 0.0001$) (Fig. 2*A*). In contrast, all three mutants significantly lost their ability to suppress S3C-induced growth compared with wild-type GRIM-19 under the same conditions. These differences in growth characteristics are not due to differences in expression levels of the proteins (Fig. 2*B*).

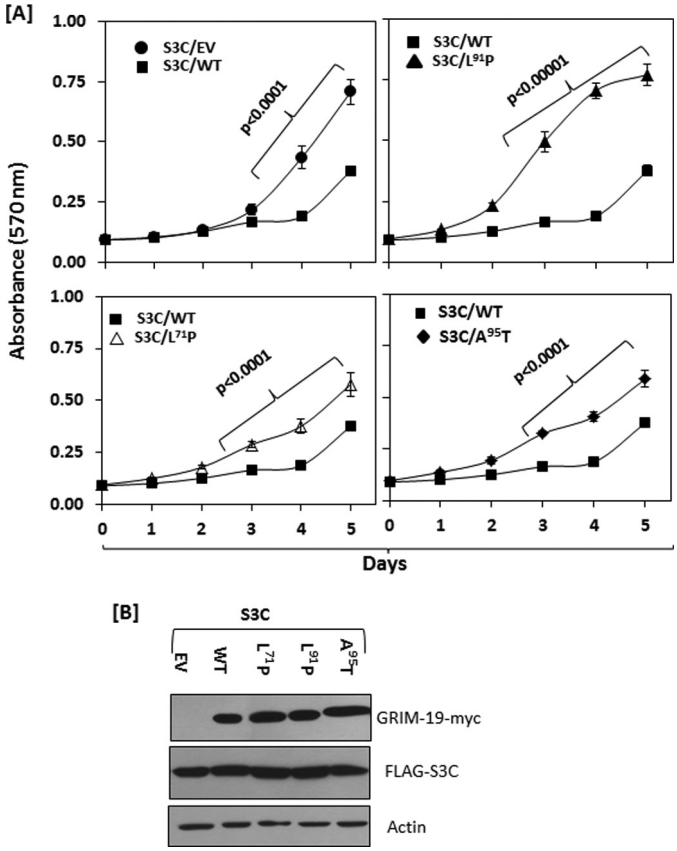

FIGURE 2. **Tumor-derived GRIM-19 mutants lost the capacity to suppress S3C-driven cell proliferation in 3Y1 cells.** *A*, stable populations of cells expressing FLAG-S3C and Myc-GRIM-19 constructs were analyzed for growth differences using sulforhodamine B dye ($n = 6$ in each case). *B*, shown is Western blot analysis of GRIM-19 mutants in 3Y1 cells. Total extracts were probed with epitope-tag-specific and actin-specific antibodies. *WT*, wild-type GRIM-19. *Error bars* indicate S.E.

Effect of GRIM-19 Mutants on S3C-induced Transformation—Because growth stimulation occurred in the presence of GRIM-19 mutants, we next determined their effects on oncogenic phenotype using two models. In the first model, 3Y1 cells expressing S3C alone or in combination with GRIM-19 mutants were used for anchorage-independent growth on soft agar media. As expected, S3C-expressing cells formed a large number of soft-agar colonies, unlike the empty vector or GRIM-19 singly transfected cells (Fig. 3*A*). S3C-dependent soft agar colony formation was robustly suppressed by GRIM-19. We then quantified and compared the differences between wild-type and mutant GRIM-19 to measure their impact on S3C-induced transformation (Fig. 3*B*). The mutants, L71P, L91P, and A95T significantly lost ($p < 0.001$, <0.008, and <0.0001, respectively) their ability to suppress S3C-induced transformation compared with wild type. The mutants alone did not have any transforming effect in these cells. In a second model, we employed a human oral squamous cell carcinoma cell line, HSC3, which expresses a very low level of GRIM-19 (23) and high basal STAT3 activity, to determine the impact of mutants on colony formation. We noted similar effects of GRIM-19 mutants on colony formation in HSC3 cells (Fig. 3*C*). However, A95T mutant was least inhibitory in 3Y1 cells, whereas the same mutant was strongest in HSC3 cells. The expression of mutants is shown in Fig. 3*D*. The A95T mutant had a lower expression than the wild-type protein in these cells. Overall, in S3C-transformed rat fibroblasts and human oral squamous carcinomas cells, GRIM-19 mutants were significantly weaker than the wild type at suppressing transformed phenotype.

Effect of GRIM-19 Mutants on S3C-induced Cell Motility—One of the major phenotypes of transformed cells is the acquisition of rapid motility. In the next experiments we examined the effects of GRIM-19 on S3C-dependent cell motility. Because HSC3 cells may have more than one genetic alteration that contributes to its transformed phenotype, it is difficult to precisely say whether all oncogenic effects are STAT3-driven. Therefore, we employed 3Y1 and HaCaT (a non-oncogenic keratinocyte) cells to study the impact of GRIM-19 mutants on S3C-dependent motility. In the initial assays, we employed 3Y1 cells expressing S3C in the presence or absence of GRIM-19 mutants. A confluent monolayer of each of these cell lines was scratched with a sterile pipette tip, and cell motility into the denuded area was monitored over time. As shown in Fig. 4*A*, very few cells moved into the denuded area in empty vector (EV)[2]-transfected cells. Several S3C-expressing cells migrated into the denuded area within 4 h. Wild-type GRIM-19 blunted S3C-induced motility. In contrast to the wild type, the L71P, L91P, and A95T mutants significantly lost their capacity to block S3C-induced motility, as evidenced by migration of cells into the denuded area. Fig. 4*B* shows quantified data from a number of plates ($n = 6$; three replicates per experiment). HaCaT cells were stably transfected with a modified S3C expression vector. The original pRc/CMV-S3C with BGH-poly(A) signals did not express in keratinocytes; hence, we replaced this sequence with a poly(A) signal sequence from *KRT-14*. After establishing stable cell lines that expressed S3C (Fig. 4*C*), they were infected with lentiviral particles coding for wild-type or mutant versions of GRIM-19. In HaCaT cells, L71P mutant expressed to a lower extent than wild type or L91P, whereas A95T mutant expressed very weakly.

In the next set of experiments migration was scored using Transwell® migration assays. 3Y1 and HaCaT cells expressing the indicated gene products were employed for this study (Fig. 4*D*). Relative to S3C-expressing cells, fewer GRIM-19-expressing cells moved into the lower chamber. In contrast, significantly higher numbers of mutant-expressing cells migrated into the lower chambers in both cell types. More importantly, both these appear to be resulting from a failure to antagonize S3C. Lastly, we investigated the impact of these mutants on IL-6-induced cell migration using HSC3 cells expressing GRIM-19 mutants in Transwell® chambers (Fig. 4*E*) given recent reports that IL-6 is a potential growth factor for many tumors (24). IL-6-stimulated cell migration was high in the EV transfectants, which was strongly suppressed by wild-type GRIM-19 ($p < 0.0001$). The mutants when compared with wild-type GRIM-19 significantly ($p < 0.002$) lost the capacity to block IL-6-induced migration.

[2] The abbreviations used are: EV, empty vector; IP, immunoprecipitation; U-STAT3, un(tyrosyl)-phosphorylated STAT3.

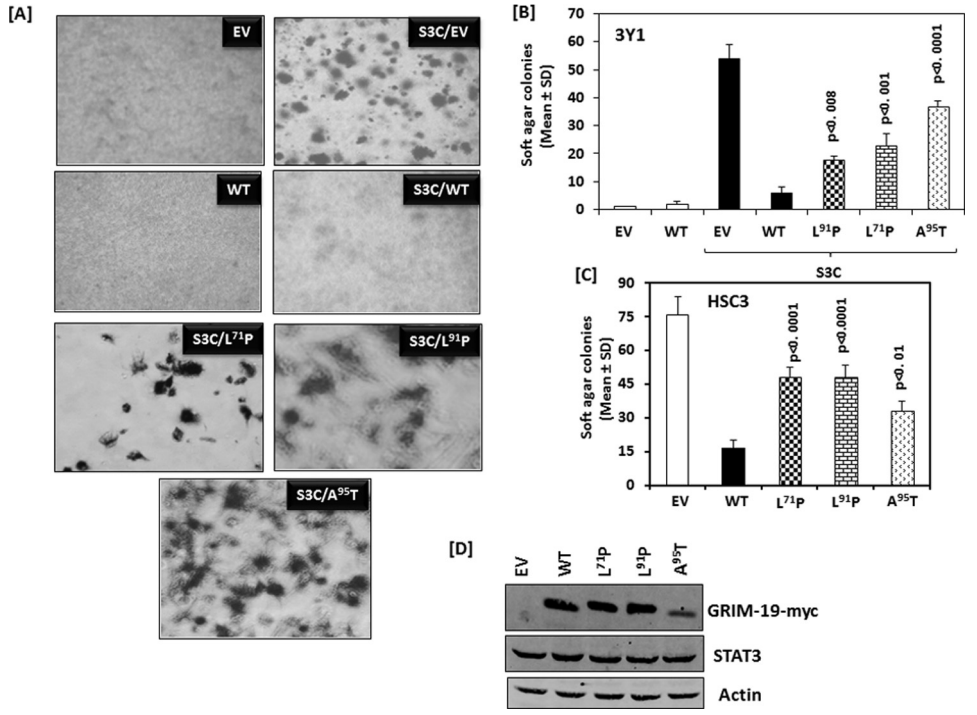

FIGURE 3. **GRIM-19 mutants fail to suppress anchorage-independent growth.** *A*, GRIM-19 inhibits S3C-induced anchorage-independent (soft agar) growth of 3Y1 cells. *B*, effects of GRIM-19 mutants on S3C-induced soft-agar colony formation ($n = 6$ plates in each case)are shown. *C*, procedures as in *B*, except the experiment was performed in an oral cancer cell line HSC3. Endogenous STAT3 in this cell line was targeted with GRIM-19 and its mutants to study the effects. *D*, shown is a Western blot analysis of the expression of GRIM-19 and its mutants in HSC3 cells. *Error bars* indicate S.E.

Anti-tumor Effects of GRIM-19 Mutants—To determine the effects of GRIM-19 mutants on tumor growth, we subcutaneously transplanted HSC3 and PC3 cells expressing these mutants into athymic nude mice (Figs. 5, *A* and *B*). We showed earlier that these cells express an extremely reduced level of endogenous GRIM-19 and high STAT3 activity (23, 25). Hence, the effects of mutants on cell growth can be readily distinguished in these cells. HSC3 cells formed relatively smaller-sized tumors unlike PC3 cells. Nonetheless, in both cell types wild-type GRIM-19 suppressed tumor formation robustly ($p < 0.001$), whereas the mutants (L71P, L91P, and A95T) were relatively weaker ($p < 0.01$) at suppressing tumor growth. Among these, L71P and L91P were the weakest growth suppressors. Relative to these mutants, A95T retained a significantly higher growth inhibitory capacity ($p < 0.05$). Thus, patient-derived mutant GRIM-19 proteins failed to suppress tumor growth.

The above experiments did not unequivocally prove whether the anti-tumor effects are directly a result of the effects of GRIM-19 on a deregulated STAT3. Because S3C-transformed HaCaT cells did not form tumors in mice consistently, we did not use them for these studies. Hence, we subcutaneously administered S3C-expressing 3Y1 cell line derivatives into nude mice. As shown in Fig. 5*C*, unlike the parent cells (which did not form any noticeable tumors), S3C-expressing 3Y1 cells formed large tumors. Wild-type GRIM-19 completely suppressed S3C-dependent tumor formation ($p < 0.0001$). The mutants, unlike the wild type, lost their ability to suppress S3C-dependent tumor formation. Specifically, L71P and L91P were the weakest of three mutants ($p < 0.005$). Although A95T mutant suppressed tumor growth, it was significantly ($p < 0.02$) weaker than wild-type GRIM-19.

Anti-metastatic Effects of GRIM-19 Mutants—We next investigated if these GRIM-19 mutants had any effect on tumor metastases. Because HSC3 cells were not metastatic and there was no other metastatic oral cancer cell line available to us at this time, to determine the anti-metastatic effects, we transduced lentiviral particles coding for GRIM-19 mutants into a metastatic PC3 cell line expressing firefly luciferase gene, so the migration of tumor cells could be monitored in real time. The tumor cells expressing different GRIM-19 mutants were orthotopically transplanted into the prostate gland of nude mice and were imaged after 45 days. Mice transplanted with empty vector-expressing PC3 cells showed high metastatic behavior as seen by the migration of cells from prostate to other parts of the body (Fig. 6*A*). In contrast, wild-type GRIM-19-expressing cells showed an extremely weak metastatic behavior. All three mutants significantly ($p < 0.02$) lost their capacity to block metastatic spread when compared with the wild type (Fig. 6*A*). A quantitative representation of luciferase signals from metastasized regions is presented in Fig. 6*B*. The expression of GRIM-19 and its mutants in these cells was verified using a Western blot analysis (Fig. 6*C*).

The GRIM-19 Mutants Fail to Suppress S3C-induced Cellular Resistance to Chemotherapeutics—Constitutive STAT3 activity causes chemoresistance (26) in the tumors. We next examined if these GRIM-19 mutations have any effect on drug sensitivity of cells. Equal numbers of 3Y1 cells expressing S3C and GRIM-19 mutants were treated with Adriamycin (100 ng/ml) for 24 h, and cell survival was monitored compared with the corresponding untreated cells (Fig. 7). The presence of S3C caused an ~60% survival of cells compared with the control EV cells. In the presence of wild type GRIM-19, cells became as

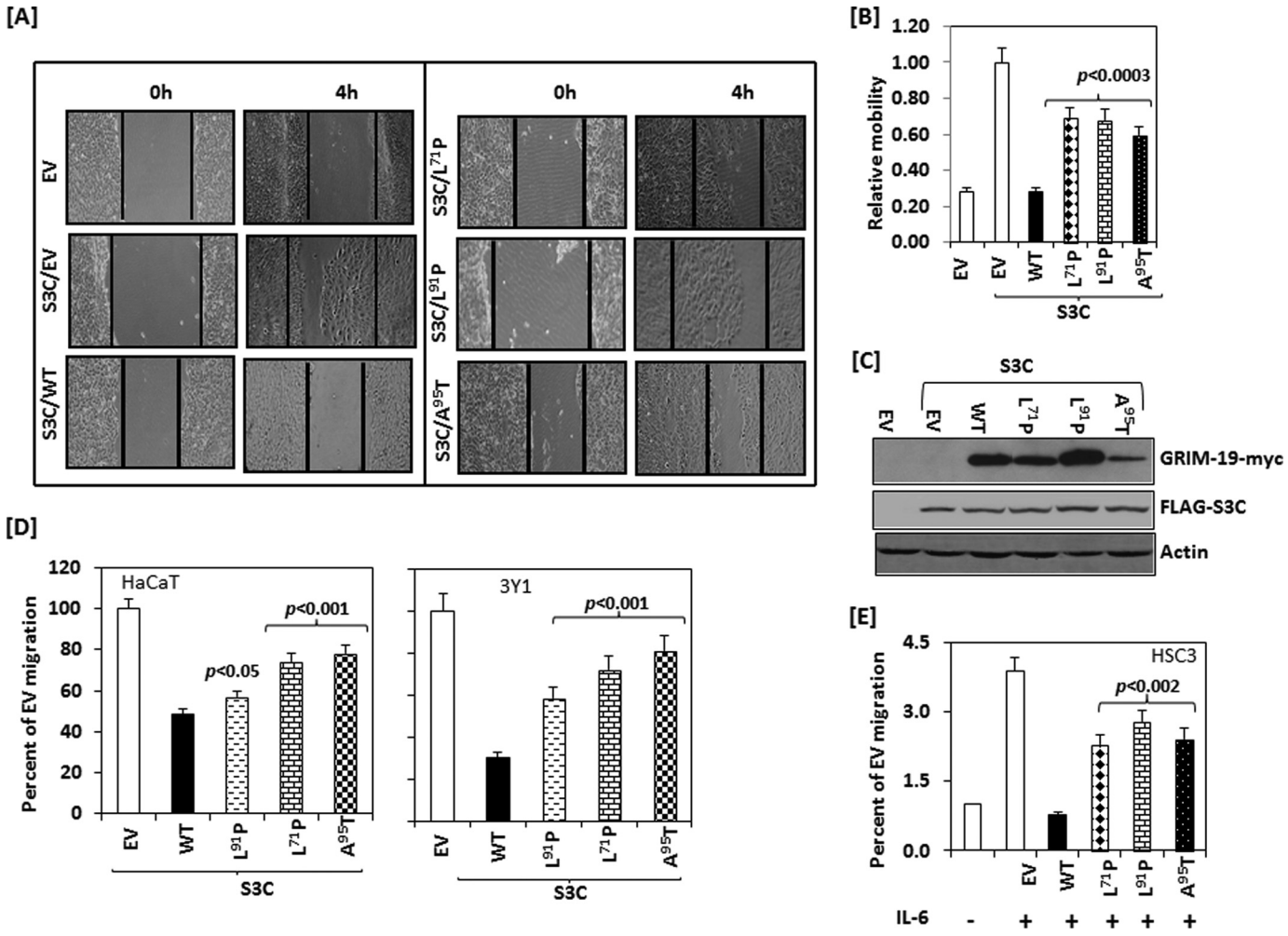

FIGURE 4. **Impact of GRIM-19 mutations on cell motility.** *A*, confluent monolayers of 3Y1 cells were scratched with a pipette tip. Movement of cells into the denuded area was monitored after 4 h. *B*, data from several plates ($n = 6$), similar to those shown in *panel A*, were quantified to determine the effect of GRIM-19 mutants on cell motility. *C*, expression of GRIM-19 mutants in HaCaT cells is shown. *D*, the Effect of GRIM-19 mutations on cell migration in Transwell® chambers is shown. The upper chambers were separated from the medium by an 8-μm polycarbonate membrane. Cells (50,000 per chamber) were loaded and inserted into wells containing DMEM with 10% serum. *p* values represent the comparison of data obtained with each mutant to those of wild type. *E*, procedures were similar to *panel D*, except that the lower chamber medium contained 1% charcoal-stripped serum supplemented with 100 ng/ml of IL-6. *Error bars* indicate S.E.

drug-sensitive as the EV cells despite the presence of S3C. All three mutants significantly lost their capacity to enhance chemosensitivity of cells compared with the wild-type GRIM-19. Thus, the loss of GRIM-19 activity (due to mutations) in the context of an oncogenic STAT3 may decrease cellular sensitivity to chemotherapeutics.

GRIM-19 Mutants Fail to Suppress STAT3-induced Gene Expression—To understand the underlying mechanisms by which GRIM-19 mutants lost their anti-STAT3 activity, we first measured the expression of STAT3-inducible genes. We performed these experiments in 3Y1 and HaCaT cell lines expressing S3C and GRIM-19 mutants. Because these cell lines represent two different species, we could only perform the quantitative PCR analysis for genes that showed STAT3 responsiveness in these cell lines. As expected, *BCL2-L1*, *DP1* (the binding partner for cell cycle regulating transcription factor E2F1), and cytoskeletal remodeling factor *CTTN1* (Cortactin 1) genes were strongly induced in cells expressing S3C in HaCaT cells (Fig. 8*A*). Wild-type GRIM-19 suppressed the expression of all three genes, comparable with levels found in the EV-transfected cells. The mutants were still able to suppress S3C-responsive gene expression, albeit not as well as the wild type. The L91P mutant was able to suppress *BCL2-L1* levels better than wild-type protein and the best mutant capable of suppressing S3C-responsive genes in HaCaT cells.

In 3Y1 cells, transcripts coding for the anti-apoptotic *Bcl2-l1* and *Ccnb1* (cyclin B1) were induced strongly by S3C, which were suppressed by wild-type GRIM-19 (Fig. 8*B*). All three mutants significantly lost their capacity to suppress S3C-inducible gene expression relative to wild-type GRIM-19. Interestingly, the L71P mutant was the only mutant that repressed *Ccnb1* better than the wild type in these cells. The basis for the repressive effect of L91P (in HaCaT) on *BCL2-L1* and L71P (in 3Y1) on *Ccnb1* is unclear at this stage. The differential effects of these mutants may be due to a post-transcriptional effect or a different chromatin niche or the regulatory elements controlling them and not due to variations in their cellular localization (supplemental Fig. S3). The wild-type and mutant proteins distributed similarly in the cytoplasmic and nuclear compartments.

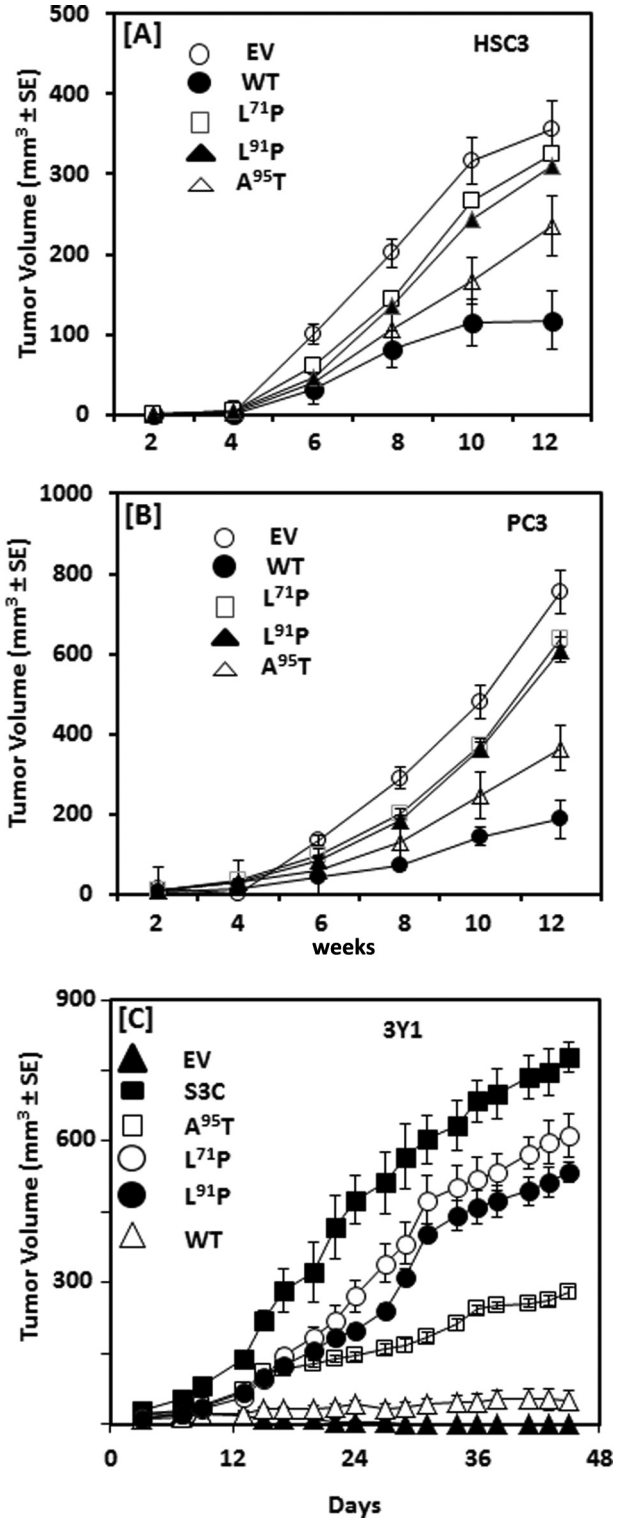

FIGURE 5. **GRIM-19 mutants are incapable of suppressing tumor formation.** *A* and *B*, HSC3 and PC3 cells (10^6/mouse) expressing various GRIM-19 mutants were transplanted into nude mice subcutaneously ($n = 10$/group), and tumor growth was quantified. *C*, impact of GRIM-19 mutants on S3C-induced tumor growth is shown. 3Y1 cells expressing GRIM-19/S3C combinations were transplanted into athymic nude mice subcutaneously ($n = 10$/group), and growth was measured. In all 3 models, mutants significantly lost their anti-tumor activity ($p < 0.001$) when compared with wild-type GRIM-19. *Error bars* indicate S.E.

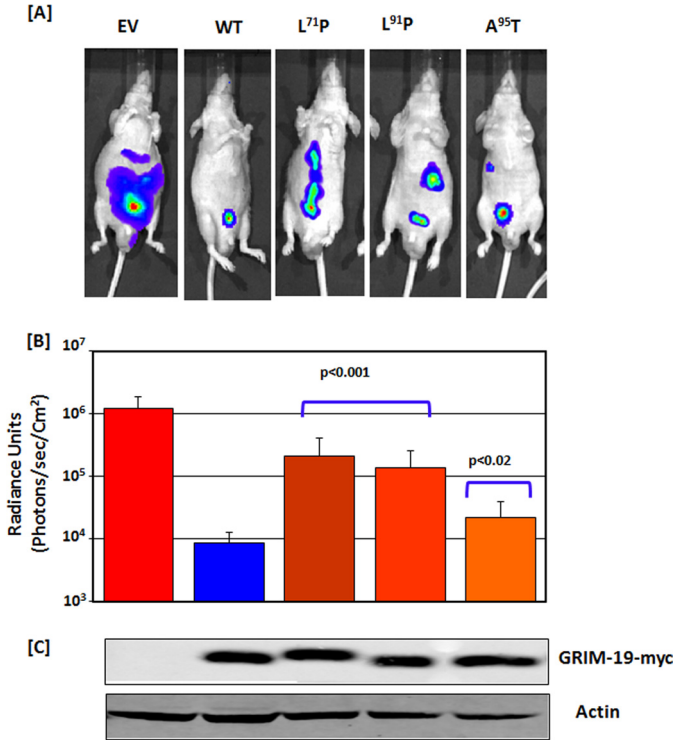

FIGURE 6. **GRIM-19 mutants lost their anti-metastatic activity.** *A*, equal numbers of metastatic PC3 cells (5×10^5 cells/mouse) expressing the different GRIM-19 mutants and firefly luciferase were orthotopically injected into prostate glands of male athymic nude mice ($n = 4$/group). Mice were monitored for metastasis after 45 days using the Xenogen IVS100 live imaging system. Representative mice from each group are shown. After anesthetizing, mice were administered 3 mg of luciferin intraperitoneally 5 min before imaging. Image acquisition settings were: Bin 8, FOV25, f1, 30-s exposure, background subtracted, flat-fielded, cosmic. *B*, quantified photon emission in the areas of interest is shown. *p* values for mutants were calculated by comparing each of them to the wild type. *C*, a Western blot analysis of GRIM-19 expression (wild type and mutants) in PC3 cells is shown. *Error bars* indicate S.E.

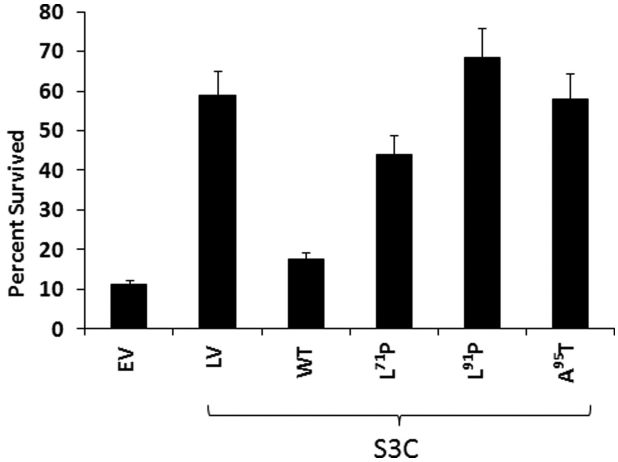

FIGURE 7. **Effects of GRIM-19 mutations on STAT3C-induced chemoresistance.** 3Y1 cells stably transfected with S3C/GRIM-19 mutations were treated with Adriamycin (100 ng/ml) for 24 h, and the percentage of surviving cells was calculated by comparing them to their respective untreated controls in each case. Each *bar* represents eight replicates in the same experiment. The mutant effects on cell survival were significantly different from the wild type ($p < 0.0001$). *Error bars* indicate S.E.

We also determined the impact of GRIM-19 mutants on the expression of certain STAT3-regulated genes in HSC3 and PC3 cells using Western blots. In HSC3 cells wild-type GRIM-19

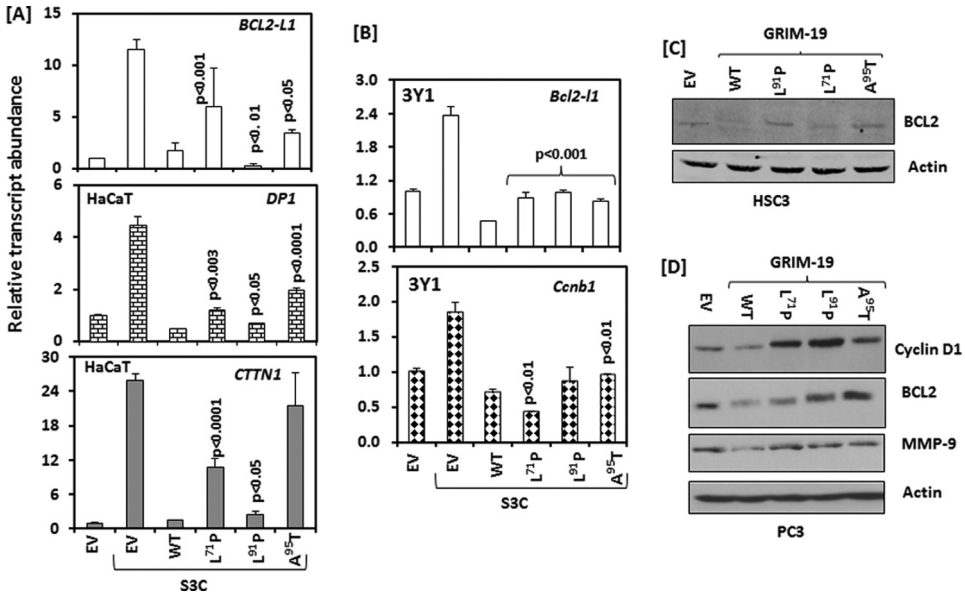

FIGURE 8. **GRIM-19 mutants are incapable of suppressing STAT3-responsive gene expression.** *A* and *B*, real time PCR analysis of the indicated transcripts in HaCaT and 3Y1 cells is shown. The *p* values were calculated by comparing data obtained with the specific mutant and wild-type GRIM-19 in each case. The effect of L91P on *Ccnb1* in 3Y1 cells is statistically borderline. *C* and *D*, Western blot analyses of the indicated STAT3-responsive proteins in HSC3 and PC3cells is shown. *p* values were calculated by comparing the data obtained with each mutant with those of wild-type protein. *Error bars* indicate S.E.

suppressed the expression of BCL2 protein, but its expression increased when GRIM-19 mutants were present (Fig. 8*C*). In PC3 cells, expression of cyclin D1, BCL2, and metastasis-associated protease MMP-9 was suppressed by wild-type GRIM-19, but the mutants were unable to block the expression of these proteins (Fig. 8*D*). Taken together, these data show a global loss of control by the tumor-derived GRIM-19 mutants over STAT3.

Defective Binding of Mutant GRIM-19 Proteins to STAT3—We next checked if the GRIM-19 mutants were capable of binding to STAT3 by co-immunoprecipitation (co-IP). Mutant and wild-type GRIM-19 proteins from 3Y1 cells were immunoprecipitated with myc-tag-specific antibodies. The IP products were probed for the presence of endogenous STAT3 using Western blotting. Indeed, all GRIM-19 mutants significantly lost their capacity to bind STAT3, unlike the wild type (Figs. 9, *A* and *B*). Similar results were obtained in other cells. Recent studies showed that STAT3 can drive transcription in the absence of phosphorylation at Tyr-705; hence, we asked if the mutants were also defective at binding to such a STAT3. To this end, we examined the interactions of mutant GRIM-19 proteins with a FLAG-tagged STAT3-Y705F mutant. Although wild-type GRIM-19 protein interacted with STAT3-Y705F mutant, GRIM-19 mutants were significantly defective (Fig. 9*C*).

Because this assay simply shows a loss of binding, it does not reflect if the mutations have functional consequences. Because GRIM-19 binds to the transactivation domain of STAT3, its inhibitory effect on transcription should involve recruitment to the enhancers of STAT3-regulated genes. We have previously shown that GRIM-19 is recruited to the promoters of STAT3-regulated genes like *Bcl2*, *Bcl2-l1*, and *Ccnd1* (21) to exert a repressive effect. Therefore, we examined if mutant GRIM-19 proteins were capable of associating with chromatin. HSC3 cells were subjected to ChIP assays with STAT3- and GRIM-19-specific antibodies (Fig. 9*D*). As an example, we used *BCL2* promoter, as it is repressed by GRIM-19 in all cell types tested and is overexpressed in primary tumors. After preparation of soluble chromatin, IP with the indicated antibodies was conducted, and DNA recovered from the IP products was subjected to PCR with *BCL2* promoter-specific primers. In EV-transfected cells, only STAT3 was present at the promoter, whereas wild-type GRIM-19 was found when STAT3 was present. In contrast, the mutant proteins weakly associated with *BCL2* promoter. To demonstrate that GRIM-19 and STAT3 are with the same promoter fragment, chromatin was chromatin-immunoprecipitated first with GRIM-19-specific (myc tag) antibodies, and the products were re-chromatin-immunoprecipitated with a STAT3-specific or a control IgG. Although the control IgG could not IP *BCL2* promoter region, the STAT3-specific antibodies could IP the *BCL2* promoter region. Although a strong signal was seen with wild-type GRIM-19, a reduced signal was observed with mutants. Altogether, these data show a severely diminished interaction of tumor-derived GRIM-19 mutant with STAT3 compromises their growth-suppressive actions.

DISCUSSION

STAT3 is a major oncogene (15) functioning downstream of many activated tyrosine kinase oncogenes, mutated, and/or overexpressed growth factor receptors in different human tumors (16). Its constitutive activity is linked to the induction of cell growth promoters like M-Ras, c-Myc, cyclin D1, cyclin B1, and DP1 and anti-apoptotic regulators like BCL2, BCL2-L1, MCL1, metastasis-promoting members of MMP family, all of which are associated with tumor initiation and progression (27). High STAT3 activity is also associated with chemoresistance (26). Although it was thought initially that only the tyrosyl-phosphorylated dimeric STAT3 was capable of driving up oncogenic gene expression (16), recent studies point out that un(tyrosyl)-phosphorylated STAT3 (U-STAT3) can also

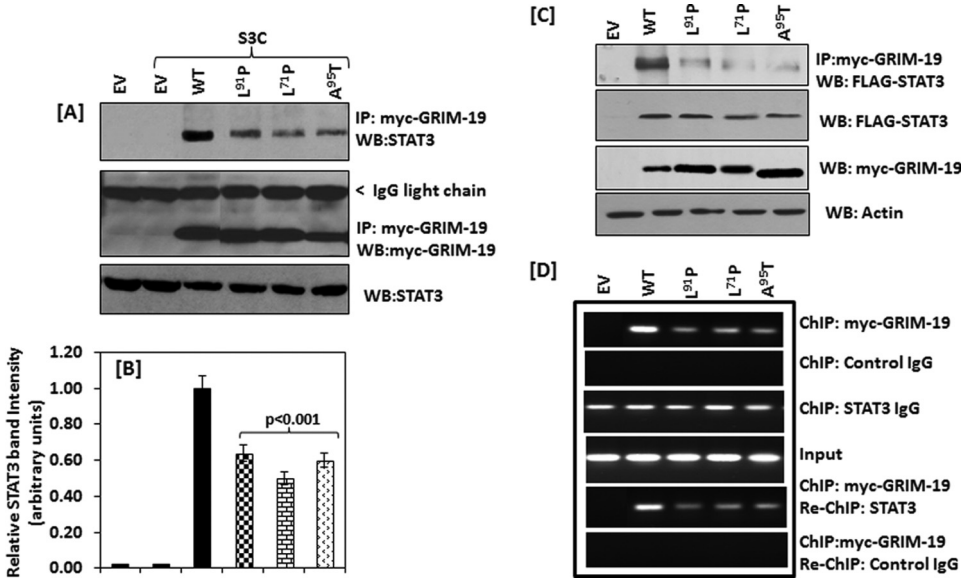

FIGURE 9. **Mutant GRIM-19 proteins weakly interact with STAT3.** *A*, shown is a co-immunoprecipitation assay for interaction of STAT3 with mutant GRIM-19 protein in 3Y1 cells. *WB*, Western blot. *B*, shown is quantified STAT3 band intensity in GRIM-19 IP products. Mean values are shown ($n = 3$ blots). Similar data were obtained with other cells. *p* values were obtained by comparing each mutant to the wild-type GRIM-19 control. *C*, interaction of U-STAT3 with GRIM-19 mutants is shown. A FLAG-tagged Y705F mutant was co-expressed along with GRIM-19 mutants in 3Y1 cells. IP and Western blot analyses were carried out using the indicated antibodies. *D*, ChIP assays for the promoter occupation of GRIM-19 mutants and STAT3 on the *BCL2* gene in HSC3 cells are shown. Soluble chromatin was immunoprecipitated using the indicated antibodies after cross-linking *in situ* with formaldehyde. The DNA recovered from the ChIP was subjected to PCR with *BCL2* promoter-specific primers. *Error bars* indicate S.E.

do so (28). Despite the extensive knowledge of the oncogenic mechanisms downstream of STAT3, it is unclear what leads to its chronic activity in cells. STAT3 mutations have been reported in certain forms of immune disorders (29–33) but not in human tumors. This leaves one possibility for constitutive STAT3 activation, *i.e.* the loss or inactivation of STAT3 inhibitors. Among these proteins are SOCS3 (which inhibit JAKs that activate STAT3) and the proteinaceous inhibitor of activated STAT3 (PIAS3). SOCS proteins are not known to block non-JAK-tyrosine kinases; hence, they cannot provide a basis for the loss of control over STAT3. In fact, SOCS3 cannot block oncogene-induced STAT3 activation (34). Furthermore, SOCS3 expression itself is STAT3-dependent and is used as marker of STAT3 activity (35). The PIAS proteins are SUMO ligases that primarily target steroid and other transcription factors (36–39). Their direct relevance to constitutively active STAT3 is largely unknown. The tumor suppressor LKB1 (STK11) is a cytoplasmic/nuclear serine/threonine kinase, defects in which cause Peutz-Jeghers syndrome in humans and animals (40). Recent studies showed that loss of function of LKB1 is associated with sporadic forms of lung, pancreatic, and ovarian cancers (41, 42). LKB1 is inactivated by two different mechanisms: (*a*) mutations in its central kinase domain or (*b*) complete loss of its expression. Inactivation of LKB1 was associated with progression of Peutz-Jeghers syndrome and transformation of benign polyps into malignant tumors. We reported earlier that LKB1 inhibited rearranged in transformation/papillary thyroid carcinoma -dependent activation of STAT3 (phosphorylation of Tyr-705) (43). The kinase domain of LKB1, but not its activity, was critical for this effect (43). In contrast to these observations, a latest study showed that inactivation of STAT3 promoted tumor growth in certain forms of human papillary thyroid cancers and those driven by the $BRAF^{V600E}$ (44). These latter observations suggest a tissue and/or cell type-specific oncogenic/tumor suppressive effects of STAT3. One possible explanation for these differential effects is the tissue-specific post-translational modifications such as acetylation, methylation, and SUMOylation the STAT proteins undergo (14). Because RET/ papillary thyroid carcinoma is not a common alteration in most human tumors and LKB1 is not expressed in all tissues, inactivation of other potential inhibitors of STAT3 may contribute to unregulated STAT3 activity and consequent ontogenesis. In this connection, GRIM-19 appears to be such a candidate, as it is expressed in all cell types.

Overexpression of GRIM-19 caused growth inhibition and apoptosis, whereas depletion of GRIM-19 levels promoted growth (11). Unlike the other known STAT3 inhibitors, basal levels of GRIM-19 are found in all mammalian cells, which further support our hypothesis that it may act as an anti-oncogene in many cell types. Consistent with this, our earliest observations showed that the vIRF1 oncoprotein of human herpesvirus 8 (KSHV) inactivates anti-tumor activity of GRIM-19 by a direct interaction (45). In addition, the SV40 T antigen and HPV-E6 oncoprotein also bind to GRIM-19 (45). The E6/E6AP complex has been shown to target p53 for degradation in cervical cancers (46). We have recently shown that GRIM-19 disrupts the E6/E6AP complex formation to protect tumor suppressor p53 (47). Thus, GRIM-19 collaborates with other tumor-suppressive pathways to enforce normal cell division. The subsequent protein-protein interaction studies by us and others identified several growth regulatory proteins as its targets, foremost of which is STAT3 (12, 13). Binding of GRIM-19 inactivated the transcriptional activity of STAT3. The Ser-727 residue located in the transactivation domain of STAT3 was necessary for exerting its anti-STAT3 effects (12). The impor-

tance of GRIM-19 to oncogenesis was further attested by our subsequent report that expression of GRIM-19 is inactivated in primary human renal cell carcinomas, which accompanied a high STAT3 transcriptional activity (10). The direct anti-oncogenic effects of GRIM-19 were shown by an inactivation of S3C-induced oncogenic transformation (21). In addition, many studies by us and others have shown a loss of GRIM-19 expression in a variety of primary human tumors (25, 48–55).

The current study identified mutations in the primary head and neck tumors of the oral cavity. This is the first documentation of functionally inactivating oncogenic mutations in GRIM-19 from solid tumors. Two GRIM-19 mutations, different from the ones shown here, were reported in Hürthle cell tumor of the thyroid (56), whose functional impact is unclear given the unexpected tumor-suppressive effect of STAT3 in thyroid tumors (44). The mutants identified here have clearly lost their ability to suppress S3C-induced tumor growth. The loss of anti-STAT3 effect appears to be global given similar data were obtained with the 3Y1 and HaCaT, both non-oncogenic cells. The validity of these data was further ascertained with a human oral cancer cell line HSC3, which expresses an extremely low level of GRIM-19 (23). In this model restoration of GRIM-19 robustly suppressed growth, whereas the mutants did not. It is important to note that these mutants themselves did not significantly alter normal cell growth in the absence of S3C. One of the mutations, L71P, is located in a region of GRIM-19 (amino acids 36–72) that was reported to bind STAT3 (13), confirming the previous observations. It should be noted that the large deletion that removed one-fourth of total protein (13) simply showed a required domain but did not prove whether that domain itself was sufficient for GRIM-19 binding to STAT3. However, the other two mutations, L91P and A95T, which also weakly interacted with STAT3, indicated STAT3 and GRIM-19 proteins interact using more than one contact sites. Thus, our conclusion based on point mutants was more robust than those arrived at by Lufei *et al.* (13). Having said, we do not know either the crystal or NMR structure of GRIM-19 to define how these mutations affect protein-protein interactions. Future structural analyses are clearly required to resolve these issues.

In addition, unlike wild-type GRIM-19, the mutants were unable to contain S3C-driven cell migration *in vitro*. This clearly appears to be independent of cell division, given these effects are observed within few hours. In agreement with these data, these mutants failed to suppress tumor metastasis *in vivo*. An observation that testifies to the enhanced metastasis in presence of GRIM-19 mutants (Fig. 6) is the overexpression of cortactin (57), a cytoskeletal actin remodeling protein (Fig. 8*A*). Phosphorylation of cortactin by Src family kinases initiates a sequential cellular dynamic process; 1) neutralizes cross-linked actin network (58), 2) enhances actin assembly *in vivo* (59), and 3) plays an essential role in the formation of podosome (59). This protein has been previously reported as a target of STAT3 (60) and is overexpressed in a number of metastatic tumors (61–65). Similarly, MMP-9, a protease involved tumor invasion, is also up-regulated in these cells (Fig. 8*D*). Wild-type GRIM-19 suppressed S3C-dependent cell survival in the presence of the drug, whereas GRIM-19 mutants were unable to block chemotherapeutic-induced cell death (Fig. 7). In the presence of wild-type protein, cell death was significantly enhanced. These observations suggest the importance of a functional GRIM-19 for enhancing tumor therapeutic response. These mutants also have significantly lost their ability to promote IFN-β-induced growth suppression (supplemental Fig. S4).

Mechanistically, GRIM-19 mutants have significantly lost their capacity to interact with STAT3 and as a result were incapable of inhibiting STAT3-driven gene expression (Fig. 8). Whereas wild-type GRIM-19 was able to associate with enhancer-bound STAT3, mutants significantly lost such capacity (Fig. 9*D*). Although multiple STAT3-inducible genes have been reported, S3C appears to induce them in a tissue- and cell-specific manner. Recent studies reported that U-STAT3 in association with the NF-κB/RelA subunit promoted oncogenic gene expression (35). Interestingly, many genes like CCNB1 and DP1 are induced by U-STAT3 (28), indicating that the inhibitory effects of GRIM-19 may extend to U-STAT3. Indeed, the mutants were also defective at binding U-STAT3 (Fig. 9*C*). One interesting aspect of the A95T is it appears to retain a slightly better ability to suppress metastasis than the others, even though it was as poor as the other mutants with respect to binding STAT3. This difference could not be due to differential cellular localization of this mutant (supplemental Fig. S3). Although it has lost its interaction with STAT3 like the others, it is quite likely A95T activity may target other factors, or its activity is controlled by other factors.

That said, some of the oncogenic effects of STAT3 are also non-transcriptional. For example, STAT3 has been shown to modulate cytoskeletal organization through stathmin (66), a protein that modulates microtubule polymerization. Other studies have shown that STAT3 is present in the mitochondrion of Pro-B cells and modulates oxidative phosphorylation (67). In this connection, the H-ras oncogene, a non-tyrosine kinase, has been shown to promote mitochondrial localization of STAT3 and modulation of oxidative phosphorylation (68). A sizable fraction of cellular GRIM-19 is also present in mitochondrion as part of electron transport chain complex I (69). *Grim-19* deletion causes early embryonic lethality due to severe dysfunction of electron transport chain complexes I and IV (70). In contrast to GRIM-19, STAT3 associated with electron transport chain complexes II and III in non-stoichiometric ratios (68). The exact effects of mitochondrial GRIM-19 and STAT3 interaction are unclear at present. Future studies should resolve these aspects. However, a recent study reported that during TNF-α-induced necroptosis RIPK1 phosphorylates Ser-727-STAT3 leading to recruitment of GRIM-19 and the transportation of STAT3 to mitochondrion in murine L929 cells (71). In this model STAT3 migration to the mitochondrion causes increased ROS production via enhanced electron transport chain activity and cell death. Thus, GRIM-19, although discovered in an IFN-regulated pathway, extends into other cytokine-induced biological responses. Consequently, GRIM-19 mutations described here may also affect several cellular functions to bring about oncogenic changes. Last but not the least, these mutations may help in predicting patient populations that might respond to chemotherapeutics in association with STAT3 inhibitors.

REFERENCES

1. Hanahan, D., and Weinberg, R. A. (2011) Hallmarks of cancer. The next generation. *Cell* **144,** 646–674
2. Kalvakolanu, D. V. (2004) The GRIMs. A new interface between cell death regulation and interferon/retinoid induced growth suppression. *Cytokine Growth Factor Rev.* **15,** 169–194
3. Dunn, G. P., Koebel, C. M., and Schreiber, R. D. (2006) Interferons, immunity, and cancer immunoediting. *Nat. Rev. Immunol.* **6,** 836–848
4. Chan, S. R., Vermi, W., Luo, J., Lucini, L., Rickert, C., Fowler, A. M., Lonardi, S., Arthur, C., Young, L. J., Levy, D. E., Welch, M. J., Cardiff, R. D., and Schreiber, R. D. (2012) STAT1-deficient mice spontaneously develop estrogen receptor α-positive luminal mammary carcinomas. *Breast Cancer Res.* **14,** R16
5. Taniguchi, T., Lamphier, M. S., and Tanaka, N. (1997) IRF1. The transcription factor linking interferon response and oncogenesis. *Biochim. Biophys. Acta* **1333,** M9–M17
6. Bidwell, B. N., Slaney, C. Y., Withana, N. P., Forster, S., Cao, Y., Loi, S., Andrews, D., Mikeska, T., Mangan, N. E., Samarajiwa, S. A., de Weerd, N. A., Gould, J., Argani, P., Moller, A., Smyth, M. J., Anderson, R. L., Hertzog, P. J., and Parker, B. S. (2012) Silencing of Irf7 pathways in breast cancer cells promotes bone metastasis through immune escape. *Nat. Med.* **18,** 1224–1231
7. Holtschke, T., Löhler, J., Kanno, Y., Fehr, T., Giese, N., Rosenbauer, F., Lou, J., Knobeloch, K. P., Gabriele, L., Waring, J. F., Bachmann, M. F., Zinkernagel, R. M., Morse, H. C., 3rd, Ozato, K., and Horak, I. (1996) Immunodeficiency and chronic myelogenous leukemia-like syndrome in mice with a targeted mutation of the ICSBP gene. *Cell* **87,** 307–317
8. Gozuacik, D., and Kimchi, A. (2006) DAPk protein family and cancer. *Autophagy* **2,** 74–79
9. Gresser, I., and Belardelli, F. (2002) Endogenous type I interferons as a defense against tumors. *Cytokine Growth Factor Rev.* **13,** 111–118
10. Alchanati, I., Nallar, S. C., Sun, P., Gao, L., Hu, J., Stein, A., Yakirevich, E., Konforty, D., Alroy, I., Zhao, X., Reddy, S. P., Resnick, M. B., and Kalvakolanu, D. V. (2006) A proteomic analysis reveals the loss of expression of the cell death regulatory gene GRIM-19 in human renal cell carcinomas. *Oncogene* **25,** 7138–7147
11. Angell, J. E., Lindner, D. J., Shapiro, P. S., Hofmann, E. R., and Kalvakolanu, D. V. (2000) Identification of GRIM-19, a novel cell death-regulatory gene induced by the interferon-β and retinoic acid combination, using a genetic approach. *J. Biol. Chem.* **275,** 33416–33426
12. Zhang, J., Yang, J., Roy, S. K., Tininini, S., Hu, J., Bromberg, J. F., Poli, V., Stark, G. R., and Kalvakolanu, D. V. (2003) The cell death regulator GRIM-19 is an inhibitor of signal transducer and activator of transcription 3. *Proc. Natl. Acad. Sci. U.S.A.* **100,** 9342–9347
13. Lufei, C., Ma, J., Huang, G., Zhang, T., Novotny-Diermayr, V., Ong, C. T., and Cao, X. (2003) GRIM-19, a death-regulatory gene product, suppresses Stat3 activity via functional interaction. *EMBO J.* **22,** 1325–1335
14. Stark, G. R., and Darnell, J. E., Jr. (2012) The JAK-STAT pathway at twenty. *Immunity* **36,** 503–514
15. Bromberg, J. F., Wrzeszczynska, M. H., Devgan, G., Zhao, Y., Pestell, R. G., Albanese, C., and Darnell, J. E., Jr. (1999) Stat3 as an oncogene. *Cell* **98,** 295–303
16. Yu, H., Pardoll, D., and Jove, R. (2009) STATs in cancer inflammation and immunity. A leading role for STAT3. *Nat. Rev. Cancer* **9,** 798–809
17. Kimura, G., Itagaki, A., and Summers, J. (1975) Rat cell line 3y1 and its virogenic polyoma- and sv40- transformed derivatives. *Int. J. Cancer* **15,** 694–706
18. Ushijima, T., Makino, H., Nakayasu, M., Aonuma, S., Takeuchi, M., Segawa, K., Sugimura, T., and Nagao, M. (1994) Presence of p53 mutations in 3Y1-B clone 1–6. A rat cell line widely used as a normal immortalized fibroblast. *Jpn. J. Cancer Res.* **85,** 455–458
19. Vogelstein, B., Lane, D., and Levine, A. J. (2000) Surfing the p53 network. *Nature* **408,** 307–310
20. Wang, X., Rosol, M., Ge, S., Peterson, D., McNamara, G., Pollack, H., Kohn, D. B., Nelson, M. D., and Crooks, G. M. (2003) Dynamic tracking of human hematopoietic stem cell engraftment using *in vivo* bioluminescence imaging. *Blood* **102,** 3478–3482
21. Kalakonda, S., Nallar, S. C., Lindner, D. J., Hu, J., Reddy, S. P., and Kalvakolanu, D. V. (2007) Tumor-suppressive activity of the cell death activator GRIM-19 on a constitutively active signal transducer and activator of transcription 3. *Cancer Res.* **67,** 6212–6220
22. Lindner, D. J., Borden, E. C., and Kalvakolanu, D. V. (1997) Synergistic antitumor effects of a combination of interferons and retinoic acid on human tumor cells *in vitro* and *in vivo*. *Clin. Cancer Res.* **3,** 931–937
23. Nallar, S. C., Kalakonda, S., Sun, P., Ohmori, Y., Hiroi, M., Mori, K., Lindner, D. J., and Kalvakolanu, D. V. (2010) Identification of a structural motif in the tumor-suppressive protein GRIM-19 required for its antitumor activity. *Am. J. Pathol.* **177,** 896–907
24. Hong, D. S., Angelo, L. S., and Kurzrock, R. (2007) Interleukin-6 and its receptor in cancer. Implications for translational therapeutics. *Cancer* **110,** 1911–1928
25. Zhang, L., Gao, L., Li, Y., Lin, G., Shao, Y., Ji, K., Yu, H., Hu, J., Kalvakolanu, D. V., Kopecko, D. J., Zhao, X., and Xu, D. Q. (2008) Effects of plasmid-based Stat3-specific short hairpin RNA and GRIM-19 on PC-3M tumor cell growth. *Clin. Cancer Res.* **14,** 559–568
26. Yue, P., and Turkson, J. (2009) Targeting STAT3 in cancer. How successful are we? *Expert Opin. Investig. Drugs* **18,** 45–56
27. Masuda, M., Wakasaki, T., Suzui, M., Toh, S., Joe, A. K., and Weinstein, I. B. (2010) Stat3 orchestrates tumor development and progression. The Achilles' heel of head and neck cancers? *Curr. Cancer Drug Targets* **10,** 117–126
28. Yang, J., Chatterjee-Kishore, M., Staugaitis, S. M., Nguyen, H., Schlessinger, K., Levy, D. E., and Stark, G. R. (2005) Novel roles of unphosphorylated STAT3 in oncogenesis and transcriptional regulation. *Cancer Res.* **65,** 939–947
29. Kumánovics, A., Perkins, S. L., Gilbert, H., Cessna, M. H., Augustine, N. H., and Hill, H. R. (2010) Diffuse large B cell lymphoma in hyper-IgE syndrome due to STAT3 mutation. *J. Clin. Immunol.* **30,** 886–893
30. Xie, L., Hu, X., Li, Y., Zhang, W., and Chen, L. (2010) Hyper-IgE syndrome with STAT3 mutation. A case report in Mainland China. *Clin. Dev. Immunol.* 2010, 289873
31. Papanastasiou, A. D., Mantagos, S., Papanastasiou, D. A., and Zarkadis, I. K. (2010) A novel mutation in the signal transducer and activator of transcription 3 (STAT3) gene, in hyper-IgE syndrome. *Mol. Immunol.* **47,** 1629–1634
32. Anolik, R., Elmariah, S., Lehrhoff, S., Votava, H. J., Martiniuk, F. T., and Levis, W. (2009) Hyperimmunoglobulin E syndrome with a novel STAT3 mutation. *Dermatol. Online J.* **15,** 16
33. Renner, E. D., Torgerson, T. R., Rylaarsdam, S., Añover-Sombke, S., Golob, K., LaFlam, T., Zhu, Q., and Ochs, H. D. (2007) STAT3 mutation in the original patient with Job's syndrome. *N. Engl. J. Med.* **357,** 1667–1668
34. Iwamoto, T., Senga, T., Naito, Y., Matsuda, S., Miyake, Y., Yoshimura, A., and Hamaguchi, M. (2000) The JAK-inhibitor, JAB/SOCS-1, selectively inhibits cytokine-induced but not v-Src induced JAK-STAT activation. *Oncogene* **19,** 4795–4801
35. Yang, J., Liao, X., Agarwal, M. K., Barnes, L., Auron, P. E., and Stark, G. R. (2007) Unphosphorylated STAT3 accumulates in response to IL-6 and activates transcription by binding to NFκB. *Genes Dev.* **21,** 1396–1408
36. Jackson, P. K. (2001) A new RING for SUMO. Wrestling transcriptional responses into nuclear bodies with PIAS family E3 SUMO ligases. *Genes Dev.* **15,** 3053–3058
37. Jiménez-Lara, A. M., Heine, M. J., and Gronemeyer, H. (2002) PIAS3 (protein inhibitor of activated STAT-3) modulates the transcriptional activation mediated by the nuclear receptor coactivator TIF2. *FEBS Lett.* **526,** 142–146
38. Junicho, A., Matsuda, T., Yamamoto, T., Kishi, H., Korkmaz, K., Saatcioglu, F., Fuse, H., and Muraguchi, A. (2000) Protein inhibitor of activated STAT3 regulates androgen receptor signaling in prostate carcinoma cells. *Biochem. Biophys. Res. Commun.* **278,** 9–13
39. Levy, C., Sonnenblick, A., and Razin, E. (2003) Role played by microphthalmia transcription factor phosphorylation and its Zip domain in its transcriptional inhibition by PIAS3. *Mol. Cell. Biol.* **23,** 9073–9080
40. Hemminki, A., Markie, D., Tomlinson, I., Avizienyte, E., Roth, S., Loukola, A., Bignell, G., Warren, W., Aminoff, M., Höglund, P., Järvinen, H., Kristo, P., Pelin, K., Ridanpää, M., Salovaara, R., Toro, T., Bodmer, W.,

Olschwang, S., Olsen, A. S., Stratton, M. R., de la Chapelle, A., and Aaltonen, L. A. (1998) A serine/threonine kinase gene defective in Peutz-Jeghers syndrome. *Nature* **391,** 184–187
41. Sato, N., Rosty, C., Jansen, M., Fukushima, N., Ueki, T., Yeo, C. J., Cameron, J. L., Iacobuzio-Donahue, C. A., Hruban, R. H., and Goggins, M. (2001) STK11/LKB1 Peutz-Jeghers gene inactivation in intraductal papillary-mucinous neoplasms of the pancreas. *Am. J. Pathol.* **159,** 2017–2022
42. Wang, Z. J., Churchman, M., Campbell, I. G., Xu, W. H., Yan, Z. Y., McCluggage, W. G., Foulkes, W. D., and Tomlinson, I. P. (1999) Allele loss and mutation screen at the Peutz-Jeghers (LKB1) locus (19p13.3) in sporadic ovarian tumours. *Br. J. Cancer* **80,** 70–72
43. Kim, D. W., Chung, H. K., Park, K. C., Hwang, J. H., Jo, Y. S., Chung, J., Kalvakolanu, D. V., Resta, N., and Shong, M. (2007) Tumor suppressor LKB1 inhibits activation of signal transducer and activator of transcription 3 (STAT3) by thyroid oncogenic tyrosine kinase rearranged in transformation (RET)/papillary thyroid carcinoma (PTC). *Mol. Endocrinol.* **21,** 3039–3049
44. Couto, J. P., Daly, L., Almeida, A., Knauf, J. A., Fagin, J. A., Sobrinho-Simões, M., Lima, J., Máximo, V., Soares, P., Lyden, D., and Bromberg, J. F. (2012) STAT3 negatively regulates thyroid tumorigenesis. *Proc. Natl. Acad. Sci. U.S.A.* **109,** E2361–E2370
45. Seo, T., Lee, D., Shim, Y. S., Angell, J. E., Chidambaram, N. V., Kalvakolanu, D. V., and Choe, J. (2002) Viral interferon regulatory factor 1 of Kaposi's sarcoma-associated herpesvirus interacts with a cell death regulator, GRIM19, and inhibits interferon/retinoic acid-induced cell death. *J. Virol.* **76,** 8797–8807
46. Huibregtse, J. M., Scheffner, M., and Howley, P. M. (1993) Localization of the E6-AP regions that direct human papillomavirus E6 binding, association with p53, and ubiquitination of associated proteins. *Mol. Cell. Biol.* **13,** 4918–4927
47. Zhou, Y., Wei, Y., Zhu, J., Wang, Q., Bao, L., Ma, Y., Chen, Y., Feng, D., Zhang, A., Sun, J., Nallar, S. C., Shen, K., Kalvakolanu, D. V., Xiao, W., and Ling, B. (2011) GRIM-19 disrupts E6/E6AP complex to rescue p53 and induce apoptosis in cervical cancers. *PLoS ONE* **6,** e22065
48. Gong, L. B., Luo, X. L., Liu, S. Y., Tao, D. D., Gong, J. P., and Hu, J. B. (2007) Correlations of GRIM-19 and its target gene product STAT3 to malignancy of human colorectal carcinoma. *Ai Zheng* **26,** 683–687
49. Zhou, A. M., Zhao, J. J., Ye, J., Xiao, W. H., Kalvakolanu, D. V., and Liu, R. Y. (2009) Expression and clinical significance of GRIM-19 in non-small cell lung cancer. *Ai Zheng* **28,** 431–435
50. Zhou, Y., Li, M., Wei, Y., Feng, D., Peng, C., Weng, H., Ma, Y., Bao, L., Nallar, S., Kalakonda, S., Xiao, W., Kalvakolanu, D. V., and Ling, B. (2009) Down-regulation of GRIM-19 expression is associated with hyperactivation of STAT3-induced gene expression and tumor growth in human cervical cancers. *J. Interferon Cytokine Res.* **29,** 695–703
51. Okamoto, T., Inozume, T., Mitsui, H., Kanzaki, M., Harada, K., Shibagaki, N., and Shimada, S. (2010) Overexpression of GRIM-19 in cancer cells suppresses STAT3-mediated signal transduction and cancer growth. *Mol. Cancer Ther.* **9,** 2333–2343
52. Hao, H., Liu, J., Liu, G., Guan, D., Yang, Y., Zhang, X., Cao, X., and Liu, Q. (2012) Depletion of GRIM-19 accelerates hepatocellular carcinoma invasion via inducing EMT and loss of contact inhibition. *J. Cell Physiol.* **227,** 1212–1219
53. Zhang, Y., Hao, H., Zhao, S., Liu, Q., Yuan, Q., Ni, S., Wang, F., Liu, S., Wang, L., and Hao, A. (2011) Down-regulation of GRIM-19 promotes growth and migration of human glioma cells. *Cancer Sci.* **102,** 1991–1999
54. Fan, X. Y., Jiang, Z. F., Cai, L., and Liu, R. Y. (2012) Expression and clinical significance of GRIM-19 in lung cancer. *Med. Oncol.* **29,** 3183–3189
55. Li, F., Ren, W., Zhao, Y., Fu, Z., Ji, Y., Zhu, Y., and Qin, C. (2012) Down-regulation of GRIM-19 is associated with hyperactivation of p-STAT3 in hepatocellular carcinoma. *Med. Oncol.* **29,** 3046–3054
56. Máximo, V., Botelho, T., Capela, J., Soares, P., Lima, J., Taveira, A., Amaro, T., Barbosa, A. P., Preto, A., Harach, H. R., Williams, D., and Sobrinho-Simões, M. (2005) Somatic and germline mutation in GRIM-19, a dual function gene involved in mitochondrial metabolism and cell death, is linked to mitochondrion-rich (Hurthle cell) tumours of the thyroid. *Br. J. Cancer* **92,** 1892–1898
57. Weed, S. A., Karginov, A. V., Schafer, D. A., Weaver, A. M., Kinley, A. W., Cooper, J. A., and Parsons, J. T. (2000) Cortactin localization to sites of actin assembly in lamellipodia requires interactions with F-actin and the Arp2/3 complex. *J. Cell Biol.* **151,** 29–40
58. Huang, C., Ni, Y., Wang, T., Gao, Y., Haudenschild, C. C., and Zhan, X. (1997) Down-regulation of the filamentous actin cross-linking activity of cortactin by Src-mediated tyrosine phosphorylation. *J. Biol. Chem.* **272,** 13911–13915
59. Tehrani, S., Tomasevic, N., Weed, S., Sakowicz, R., and Cooper, J. A. (2007) Src phosphorylation of cortactin enhances actin assembly. *Proc. Natl. Acad. Sci. U.S.A.* **104,** 11933–11938
60. Du, X. L., Yang, H., Liu, S. G., Luo, M. L., Hao, J. J., Zhang, Y., Lin, D. C., Xu, X., Cai, Y., Zhan, Q. M., and Wang, M. R. (2009) Calreticulin promotes cell motility and enhances resistance to anoikis through STAT3-CTTN-Akt pathway in esophageal squamous cell carcinoma. *Oncogene* **28,** 3714–3722
61. Patel, A. S., Schechter, G. L., Wasilenko, W. J., and Somers, K. D. (1998) Overexpression of EMS1/cortactin in NIH3T3 fibroblasts causes increased cell motility and invasion *in vitro*. *Oncogene* **16,** 3227–3232
62. Li, Y., Tondravi, M., Liu, J., Smith, E., Haudenschild, C. C., Kaczmarek, M., and Zhan, X. (2001) Cortactin potentiates bone metastasis of breast cancer cells. *Cancer Res.* **61,** 6906–6911
63. Rothschild, B. L., Shim, A. H., Ammer, A. G., Kelley, L. C., Irby, K. B., Head, J. A., Chen, L., Varella-Garcia, M., Sacks, P. G., Frederick, B., Raben, D., and Weed, S. A. (2006) Cortactin overexpression regulates actin-related protein 2/3 complex activity, motility, and invasion in carcinomas with chromosome 11q13 amplification. *Cancer Res.* **66,** 8017–8025
64. Buday, L., and Downward, J. (2007) Roles of cortactin in tumor pathogenesis. *Biochim. Biophys. Acta* **1775,** 263–273
65. Li, X., Zheng, H., Hara, T., Takahashi, H., Masuda, S., Wang, Z., Yang, X., Guan, Y., and Takano, Y. (2008) Aberrant expression of cortactin and fascin are effective markers for pathogenesis, invasion, metastasis, and prognosis of gastric carcinomas. *Int. J. Oncol.* **33,** 69–79
66. Ng, D. C., Lin, B. H., Lim, C. P., Huang, G., Zhang, T., Poli, V., and Cao, X. (2006) Stat3 regulates microtubules by antagonizing the depolymerization activity of stathmin. *J. Cell Biol.* **172,** 245–257
67. Wegrzyn, J., Potla, R., Chwae, Y. J., Sepuri, N. B., Zhang, Q., Koeck, T., Derecka, M., Szczepanek, K., Szelag, M., Gornicka, A., Moh, A., Moghaddas, S., Chen, Q., Bobbili, S., Cichy, J., Dulak, J., Baker, D. P., Wolfman, A., Stuehr, D., Hassan, M. O., Fu, X. Y., Avadhani, N., Drake, J. I., Fawcett, P., Lesnefsky, E. J., and Larner, A. C. (2009) Function of mitochondrial Stat3 in cellular respiration. *Science* **323,** 793–797
68. Gough, D. J., Corlett, A., Schlessinger, K., Wegrzyn, J., Larner, A. C., and Levy, D. E. (2009) Mitochondrial STAT3 supports Ras-dependent oncogenic transformation. *Science* **324,** 1713–1716
69. Fearnley, I. M., Carroll, J., Shannon, R. J., Runswick, M. J., Walker, J. E., and Hirst, J. (2001) GRIM-19, a cell death regulatory gene product, is a subunit of bovine mitochondrial NADH:ubiquinone oxidoreductase (complex I). *J. Biol. Chem.* **276,** 38345–38348
70. Huang, G., Lu, H., Hao, A., Ng, D. C., Ponniah, S., Guo, K., Lufei, C., Zeng, Q., and Cao, X. (2004) GRIM-19, a cell death regulatory protein, is essential for assembly and function of mitochondrial complex I. *Mol. Cell. Biol.* **24,** 8447–8456
71. Shulga, N., and Pastorino, J. G. (2012) GRIM-19-mediated translocation of STAT3 to mitochondria is necessary for TNF-induced necroptosis. *J. Cell Sci.* **125,** 2995–3003